

The Effect of Ormosil Matrix Composition and Alkaline Earth Metal Doping on the Photochromic Response of Ormosil-Phosphotungstate Films

*Elias P. Ferreira Neto,^a Mateus B. Simões,^a Julia C. Noveletto,^b Jean M. S. C. Yabarrena,^a Sajjad Ullah^c and Ubirajara P. Rodrigues Filho^{*a}*

^aInstituto de Química de São Carlos, Universidade de São Paulo, 13560-970 São Carlos-SP, Brazil

^bDepartamento de Engenharia de Materiais, Escola de Engenharia de São Carlos, Universidade de São Paulo, 13560-120 São Carlos-SP, Brazil

^cInstitute of Chemical Sciences, University of Peshawar, 25120 Peshawar, KP Pakistan

In this study, polyoxometallate based hybrid photochromic materials were prepared by incorporating phosphotungstate anion, $PW_{12}O_{40}^{3-}$, (PW) in hybrid tetraethyl orthosilicate and (3-glycidylxypropyl)trimethoxysilane TEOS-GPTMS derived organomodified silicates (Ormosil) matrices by sol-gel method and the resulting materials were used to prepare multilayer films by dip-coating method. The effect of alkaline earth metal cations doping and matrix composition (%GPTMS) on the photochromic response of the hybrid films was studied in details. GPTMS, after undergoing ring opening reaction, leads to the formation of chelating sites (diol and ether functionalities) which helps in anchoring of cations, which in turn interacts with phosphotungstate anions and favors their incorporation in the hybrid films. For a fixed concentration of GPTMS, the cation-phosphotungstate electrostatic interaction and hence the photochromic response of the films follow the order $Mg^{2+} < Ca^{2+} < Sr^{2+} < Ba^{2+}$, thereby, indicating that larger cations interact more strongly with the heteropolyanions. The presence of these cations and GPTMS concomitantly leads to increased incorporation of phosphotungstic acid hydrate (HPW) in the films, resulting in a significant enhancement of the photochromic response.

Keywords: Ormosil, phosphotungstic acid, alkaline earth metals, photochromism, sol-gel

Introduction

Photochromic materials present interesting properties related to light-induced changes in optical absorption leading to reversible coloration/discoloration upon exposure to light.¹⁻³ Great attention has been dedicated to research on photochromic materials due to their potential applications in optical lenses, smart windows, optical memory devices UV sensors, counterfeit devices, among others.²⁻⁸

Polyoxometalates (POMs) are discrete metal-oxide nanoclusters^{9,10} which exhibit promising photochromic behavior. Such photochromic behavior is based on the photo-induced formation of mixed valence colored compounds in the presence of electron/proton donors.¹¹⁻¹³ However, in order to prepare functional photoactive materials, the highly soluble POMs need to be incorporated into suitable

solid matrices, such as polymers,¹⁴⁻¹⁶ inorganic oxides¹⁷⁻¹⁹ or hybrid organic-inorganic materials.²⁰⁻²² Additionally, most practical applications require photochromic materials to be applied as coatings or thin films.

Sol-gel synthesis is an easy and versatile strategy for the preparation of such photochromic coatings which allows effective incorporation of photoactive molecules such as POMs in sol-gel derived matrices using mild reaction conditions.^{3,23} Hybrid organic-inorganic matrices are good candidates for the preparation of such functional materials as they may combine the advantages of both polymeric and ceramic materials.^{24,25} For instance, we have recently reported the preparation of uniform, adherent and transparent hybrid photochromic and photocatalytic coatings by incorporation of phosphotungstate ($PW_{12}O_{40}$), the Keggin POMs, in organically modified silicate (Ormosils) matrices. The hybrid matrix materials were prepared by sol-gel method using tetraethyl orthosilicate (TEOS) and (3-glycidylxypropyl)trimethoxysilane

*e-mail: uprf@iqsc.usp.br

(GPTMS) as matrix-forming precursors.^{21,26} However, the weak interaction between the hybrid matrix and the Keggin heteropolyanions resulted in lower incorporation of the photoactive species in the films which led to the low photochromic response of these dip-coated films. Such limitations could be overcome by modification of the Ormosil networks with positively charged alkylammonium groups,²¹ which are known to interact strongly with POMs.²⁷ Interestingly, a similar effect could be achieved by simple concomitant addition of Zn²⁺ cations during sol-gel synthesis, leading to the preparation of highly photochromic Ormosil-polyoxometalate films.²⁸

While the interaction between organic cations and POMs in photochromic materials has been studied and exploited by several authors,²⁹⁻³³ little attention has been given to the use of inorganic ions, despite the fact that these inorganic ions greatly affect the crystallization and self-assembly of POM nanostructures.³⁴⁻³⁷ In the present study, we report the preparation of TEOS-GPTMS-phosphotungstic acid hydrate (HPW) hybrid films doped with alkaline-earth divalent cations (Mg²⁺, Ca²⁺, Sr²⁺ and Ba²⁺). A systematic study of the role of hybrid matrix composition and the presence of the doping cations in the film assembly (POM incorporation) and photochromic response of the resulting Ormosil-polyoxometalate coatings is presented. We demonstrate how the interaction between the organic functionalities, cations and phosphotungstate polyoxoanions can be exploited to significantly enhance and effectively tune the photochromic response of the hybrid films. From application point of view, such control of film architecture and photochromic response might be of great importance for design of functional photochromic coatings.

Experimental

Chemicals

Phosphotungstic acid hydrate (HPW), tetraethylorthosilicate (TEOS, 98%) and (3-glycidyloxypropyl)trimethoxysilane (GPTMS, 98%) were purchased from Sigma-Aldrich (USA). MgCl₂·6H₂O, CaCl₂·2H₂O, SrCl₂·6H₂O and BaCl₂·6H₂O were purchased from Synth (Brazil). Ethanol (99.3%) was supplied by QHEMIS (Brazil). All the reagents and solvents were used as received and without further purification.

Material synthesis and film preparation

Hybrid TEOS-GPTMS-HPW films were prepared based on our previously reported sol-gel method for the preparation of Ormosil-phosphotungstate films.^{21,26,28}

The sol-gel derived films were prepared by the addition of phosphotungstic acid and the chosen doping cations to an ethanolic solutions containing the silicon alkoxides precursors, TEOS and GPTMS. GPTMS content of the hybrid materials varied from 0 to 80% of total silicon alkoxide molar amount. The compositions of the prepared samples are summarized in Table 1.

Table 1. Composition of the sols used in the preparation of hybrid Ormosil-phosphotungstate films

Sample code ^a	HPW / mmol	TEOS / mmol	GPTMS / mmol	M ²⁺ Cl ₂ / mmol
Und0	0.75	17	0	–
Und20	0.75	13.6	3.4	–
Und40	0.75	10.2	6.8	–
Und60	0.75	6.8	10.2	–
Und80	0.75	3.4	13.6	–
Ba0	0.75	17	0	0.2 BaCl ₂
Ba20	0.75	13.6	3.4	0.2 BaCl ₂
Ba40	0.75	10.2	6.8	0.2 BaCl ₂
Ba60	0.75	6.8	10.2	0.2 BaCl ₂
Ba80	0.75	3.4	13.6	0.2 BaCl ₂
Sr80	0.75	3.4	13.6	0.2 SrCl ₂
Ca80	0.75	3.4	13.6	0.2 CaCl ₂
Mg80	0.75	3.4	13.6	0.2 MgCl ₂

^aSample codes refer to the type of doping cation added and GPTMS content of the sample (e.g., sample Ba40: Ba²⁺ doped sample prepared using 60% TEOS and 40% GPTMS).

The TEOS and GPTMS were firstly dissolved in 25 mL of ethanol in a polypropylene beaker, followed by addition of 25 mL of freshly prepared HPW ethanolic solution under magnetic stirring. In this procedure, HPW plays the additional role of acid catalyst of the hydrolysis and condensation reactions of TEOS and GPTMS. After homogenization, 825 μL of M²⁺Cl₂ 0.242 mol L⁻¹ aqueous solution (M²⁺ = Mg²⁺, Ca²⁺, Sr²⁺ or Ba²⁺) or deionized water (in the case of undoped samples) was added and the resulting mixture was kept under magnetic stirring for 15 min. The obtained sol was used to deposit thin films on soda-lime glass slides (Bioslide Technologies, USA) by dip-coating method. The glass substrates were cleaned by immersing the glass substrates in a cleaning solution composed of NH₄OH:H₂O₂:H₂O in 1:1:5 volume ratio at 70 °C for 2 h, followed by rinsing with copious amount of deionized water and drying under a steam of nitrogen. Dip-coating film deposition was carried out using a disc elevator MA-765 Marconi (Piracicaba, SP, Brazil) with ascending and descending speed adjusted at 150 mm min⁻¹. Each film was prepared by 10 immersion cycles and dried

under ambient atmosphere (relative humidity $55 \pm 10\%$, temperature 292 ± 3 K).

Characterization techniques

Fourier transform infrared (FTIR) spectra were collected at transmission mode with a Shimadzu Spectrophotometer (model IRAffinity 1) directly from films deposited on silicon plates. Spectra were recorded, using air as blank reference, from $4000\text{--}400$ cm^{-1} , 4 cm^{-1} of resolution and average of 32 scans.

X-ray diffraction (XRD) was carried out using a Bruker Diffractometer (model D8 Advance) equipped with a high resolution energy-dispersive LINXEYE EXE detector. Grazing incident diffraction was applied to assess the films. X-ray diffraction patterns were collected from $3\text{--}50^\circ$ with an incident angle fixed in 5° , scan step mode of $0.03^\circ \text{min}^{-1}$ and counting time of 0.6 s *per* step. Ni-filtered $\text{Cu K}\alpha$ radiation ($\lambda = 1.54056$ Å) were applied at 40 mA and 40 kV.

X-ray fluorescence (XRF) analysis were carried out using a benchmark energy dispersive MiniPal4 (PANalytical) spectrometer equipped with a rhodium tube as X-ray source. All the measurements were acquired after a total measurement time of 840 seconds under He atmosphere. Tungsten and barium X-ray fluorescence intensities were determined by peak fitting of $\text{W L}\alpha$ and $\text{Ba L}\alpha$ using Omnic standardless analysis package (PANalytical).

Photochromism experiments

The photochromic properties of the hybrid films were evaluated by monitoring changes in the visible light electronic absorption spectra after exposure to UV-B light. Irradiation was carried out using a 16S Solar Light Simulator Xe arc lamp (Solar Light Co., USA). The sample-to-lamp distance was 7.3 cm and the UV light spot diameter was 1 cm. The thermal visible radiations ($\lambda > 430$ nm) were filtered out by internal filters. Electronic absorption spectra were collected immediately after irradiation with a USB 4000 spectrometer (Ocean Optics, FL, U.S.A.) equipped with a P400-2 UV/Vis optical fiber and an LS1 tungsten halogen lamp. Sample films were vertically positioned (perpendicular to the light beam) in a home-made aluminum sample-holder. The spectra of each sample film were measured using the non-irradiated film itself as a blank in order to have the light scattering of the films compensated. As a measure of the photochromic response of the films, the integrated area of the intervalence charge transfer (IVCT) absorption band ($600\text{--}800$ nm) was measured from the

absorption spectra. The reversibility and stability of the photochromic response of the hybrid films were evaluated by alternatively exposing the film first to UV irradiation for 10 min and then to air/ O_2 for 24 h (in dark) for up to 10 times. The electronic absorption spectra of the films after UV illumination (10 min) and after complete bleaching (12 h) were measured during each cycle.

Results and Discussion

Characterization by FTIR analysis

FTIR is a powerful technique to study the incorporation of both organic functionalities and HPW in the obtained Ormosil films. Figure 1 presents the FTIR spectra of the undoped films prepared without (Und0) and with the highest content of GPTMS (Und80). The spectra of both samples show a broad band around 3400 cm^{-1} , assigned to the stretching vibrational mode of --OH groups from silanol (Si--OH) residues. However, --OH groups from adsorbed and entrapped water in the silica matrix and around HPW polyoxoanion may also contribute to this band. Unlike the spectrum of Und0, the spectrum of the Und80 sample shows a set of bands at around $3000\text{--}2800$ cm^{-1} . These bands arise from the C--H stretching vibration of the CH_2 groups of the organic modifier, as well the CH_2 and CH_3 groups from entrapped ethanol.³⁸

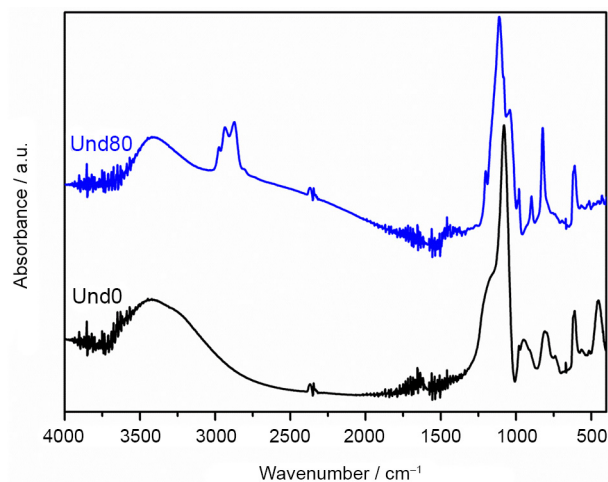


Figure 1. FTIR spectra of the undoped Ormosil films without GPTMS (Und0) and with the highest concentration of GPTMS (Und80).

Significant differences arise in the region under 1300 cm^{-1} with the increase in GPTMS content of both the undoped and Ba^{2+} -doped samples (Figure 2). Strong absorbance bands observed around $1200\text{--}1020$ cm^{-1} region are attributed to Si--O--Si vibrational modes, confirming the formation of silica network. The weaker absorbance

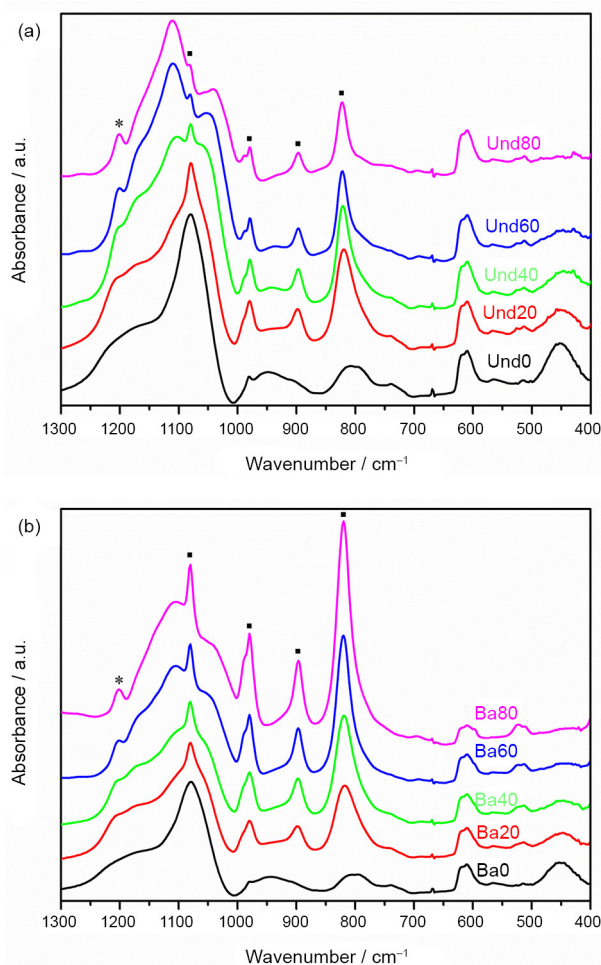


Figure 2. The low wavenumber region of FTIR spectra of the undoped (a) and Ba²⁺-doped (b) Ormosil-phosphotungstate films prepared with different concentrations of GPTMS (see Table 1). The characteristic bands of Keggin phosphotungstate are marked with (■).

bands observed under 850 cm⁻¹ are also related to the vibrational modes of Si–O and Si–O–Si groups, as well Si–OH fragments.³⁸ It is important to note that a new band appears in the spectra of GPTMS-containing samples at around 1190–1140 cm⁻¹ which is assigned to the asymmetric stretching of the C–O bonds. This C–O bond is introduced by the incorporation of GPTMS as organic modifiers groups.³⁹ Another important feature is the appearance of a discrete band in 1200 cm⁻¹ (marked with an asterisk) as we increase GPTMS concentration. This band is related to the C–O–C stretching mode.⁴⁰ Furthermore, the characteristic band due to the epoxy ring of GPTMS at 1260 cm⁻¹ is not observed. Absence of this characteristic band of epoxy ring at 1260 cm⁻¹ and the appearance of new bands due to C–O–C bond is a strong indicative that GPTMS undergoes ring opening reactions, leading to the formation of diol and ether functionalities upon hydrolysis and alcoholysis, or oligomers of polyethylene oxide (PEO) upon ring opening polymerization of the epoxy groups.^{40–42} The possible

reactions during the GPTMS ring opening are shown in Figure 3.

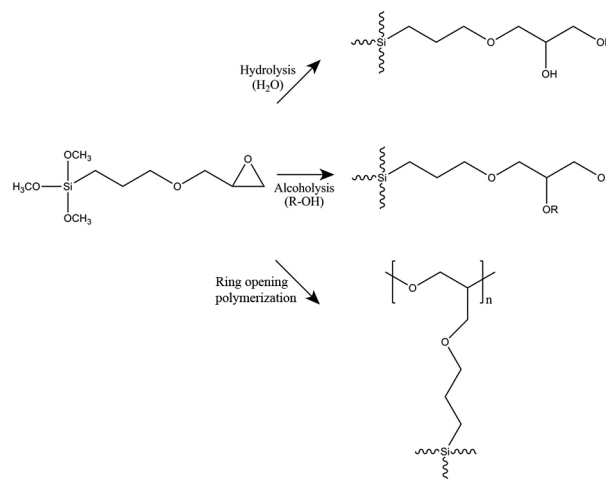


Figure 3. Schematic representation of the ring opening of epoxy groups of GPTMS (adapted from reference 42).

Finally, FTIR analysis confirms the presence of HPW in the hybrid films. The Keggin structure of heteropoly acid presents well defined and characteristics bands (marked as ■) at 1079, 979, 897 and 821 cm⁻¹ assigned to the P–O_a, W=O_d, W–O_b–W and W–O_c–W vibrational modes, respectively.⁴³ Relative absorbance of these bands is higher for the doped samples, suggesting that addition of doping cations leads to higher incorporation of HPW in the films. Such behavior was further investigated by XRF analysis as discussed later.

Characterization by XRD analysis

Since crystallization of HPW has been previously shown to suppress the photochromic response of HPW based composite materials,¹⁷ structural characterization of the prepared samples by powder XRD was carried out to understand their photochromic behavior. XRD diffractograms, for both the undoped and barium-doped samples (Figure 4) show that the GPTMS concentration strongly influences the dispersion, affinity, and crystallization of the HPW inside the matrix. Distinct diffraction peaks are observed in the diffractograms of pure inorganic SiO₂ samples (0% GPTMS), indicating crystallization of phosphotungstic acid hydrates polymorphs^{44,45} and/or their corresponding barium salts.^{46,47} The diffraction peaks start to disappear upon introduction of GPTMS into the matrix, indicating that the resulting hybrid Ormosil matrix inhibits HPW crystallization,⁴⁸ leading to a homogeneous dispersion of the heteropolyanions in the hybrid films. Furthermore, a broad peak at 2θ < 10° is observed in the diffractograms

of the Ormosil-phosphotungstate films. Such feature in the X-ray diffractograms was already observed for powder samples of Ormosil-phosphotungstate composites and is related to the formation of ordered domains inside the hybrid organosilicate network, as discussed in our previous study.²¹

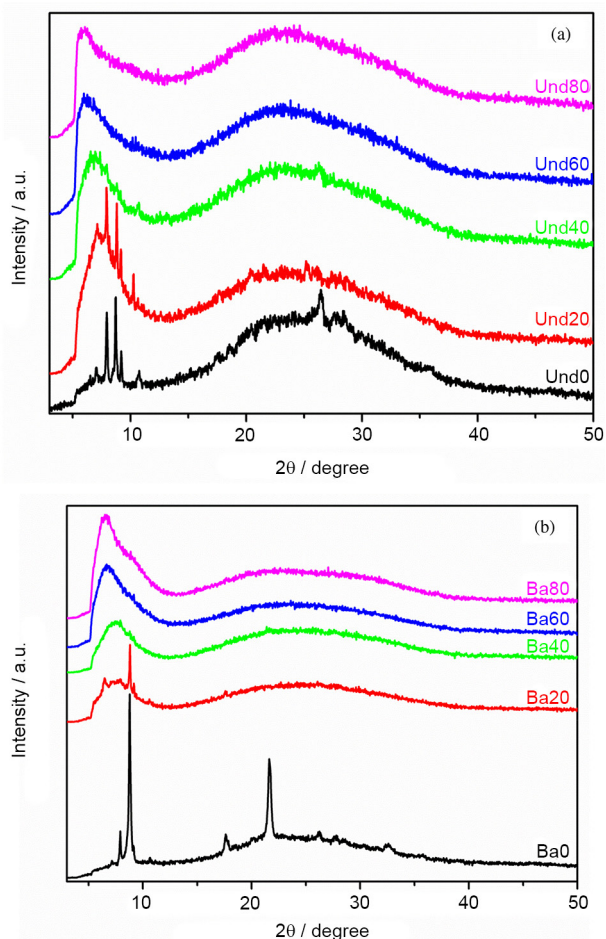


Figure 4. Diffractogram of the undoped (a) and Ba²⁺-doped (b) Ormosil films with different concentration of GPTMS.

Photochromic behavior of the hybrid films

Photochromic behavior of the hybrid films was studied by following visible light absorption changes upon exposure of the samples to UV radiation. Figure 5a shows the intensity of the broad absorption bands increases as function of UV exposure time. Such bands indicate the formation of photoreduced phosphotungstate species (e.g., $\text{PW}_{12}\text{O}_{40}^{4-}$ and $\text{PW}_{12}\text{O}_{40}^{5-}$) and are assigned to d-d (400–550 nm) and IVCT (600–800 nm) transitions.^{11–13} These changes in visible light absorption leads to photo-induced coloration of the films, which acquire a dark bluish color (Figure 5b). The coloration process is reversible and the films bleaches at room temperature due to re-oxidation

of polyoxometalate species by oxygen present in air, as demonstrated by photochromic response decay curve (Figure 5c). Furthermore, the coloration/discoloration cycles (Figure 5d) reveal stable photochromic response, with only slight decrease after repeated cycles.

Effect of the hybrid matrix composition and doping cations on the POM content and photochromic response of the hybrid films

The impact of the hybrid matrix composition (i.e., %GPTMS) and cation doping on the photochromic response of the films was evaluated by determining the integrated area of IVCT absorption band (600–800 nm). Figure 6 shows the variation of photochromic response of the undoped and Ba²⁺-doped films as function of GPTMS percentage. In both cases, the films prepared without the addition of GPTMS do not present photochromic response. Such behavior is probably related to the crystallization of HPW in the SiO₂ films, as evidenced by XRD analysis.

Upon incorporation of GPTMS at percentages higher than 20%, Ba²⁺-doped and undoped films present contrasting behavior; the photochromic response of the Ba²⁺-doped films enhances while that of the undoped samples slightly diminishes upon increasing the GPTMS content by more than 20% (Figure 6). Ba²⁺-doped sample (Ba80) presented photochromic response up to seven times higher than the most photoactive undoped sample (Und20). Thus, photochromic response of the hybrid TEOS-GPTMS-HPW dip-coated films can be enhanced by addition of Ba²⁺ cations and such enhancement can be tuned by changing the GPTMS content (Figure 6).

Similar but less pronounced effects were achieved by doping with other alkaline-earth cations. Figure 7 compares the photochromic response of both undoped and cations-doped (Mg²⁺, Ca²⁺, Sr²⁺ or Ba²⁺) films as function of UV exposure time, fixing the amount of GPTMS at 80% in all cases. The observed photochromic response followed the order: undoped < Mg²⁺ < Ca²⁺ < Sr²⁺ < Ba²⁺. It is evident that larger cations (Sr²⁺, Ba²⁺) enhance the photochromic response of the films more effectively than smaller ones, suggesting a correlation between ionic size of the dopants and the properties of the resulting material as analyzed below.

Electrostatic interaction between polyoxoanions and cations are known to strongly affect the assembly of POMs-based materials.^{34,35,49} In the specific case of Ormosil-phosphotungstate nanocomposites, hybrid matrix composition and the presence of Zn²⁺ doping cations were shown to influence the incorporation of polyoxometalate species in dip-coated films and consequently their

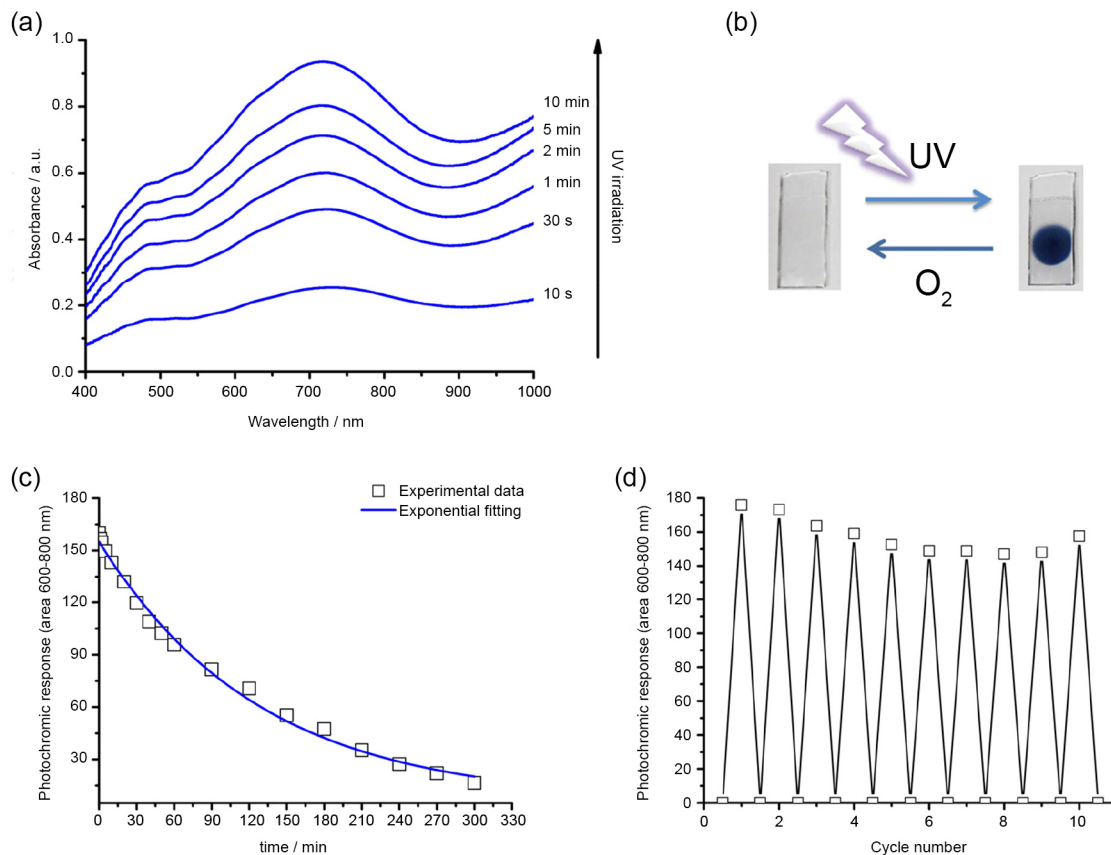


Figure 5. Photochromic behavior of the Ba^{2+} -doped hybrid films (Ba80): increase in absorptions bands of photoreduced phosphotungstate species as function of UV exposure time (a); digital photograph showing the hybrid film turning blue upon UV-B illumination and colourless upon air oxidation in dark (b); photochromic response decay curve showing the decrease in area of IVCT band (600-800 nm) upon exposure to air/ O_2 in dark (c) and reversible and stable photochromic response of the hybrid films (d). The light and dark cycles shown in (d) were performed *ex situ* by first exposing the film to UV radiation for 10 min and then allowing the color to bleach to complete discoloration during 24 h in dark.

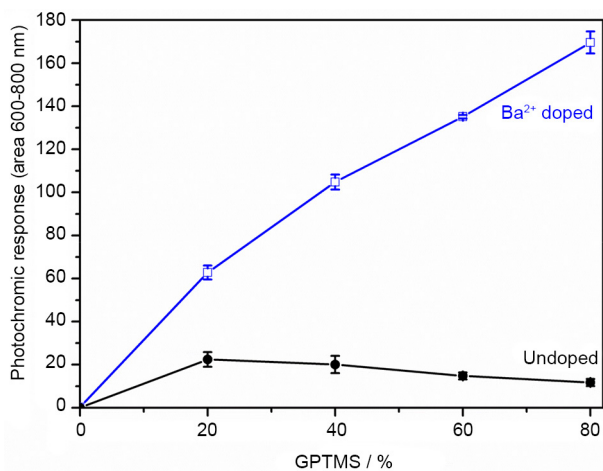


Figure 6. Photochromic response of Ba^{2+} -doped and undoped films as function of GPTMS percentage. The UV illumination time was 10 min in each case.

photochromic response.^{21,28} XRF analysis was employed to evaluate incorporation of phosphotungstate and Ba^{2+} in the hybrid films (Figure 8) by monitoring $\text{W L}\alpha$ and $\text{Ba L}\alpha$ fluorescence intensity. Barium incorporation in the Ba^{2+} -

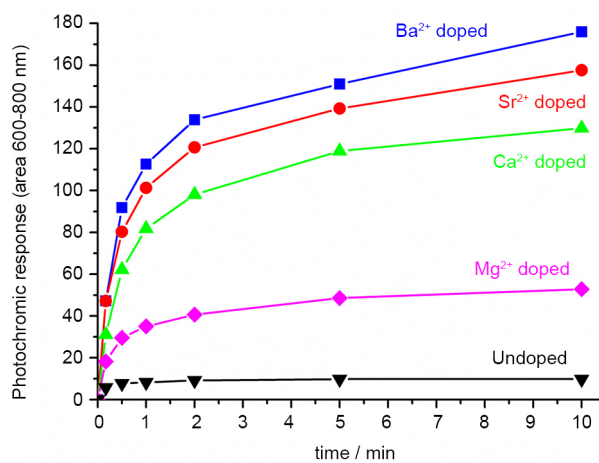


Figure 7. The photochromic response of the hybrid films (M80) with 80% GPTMS as function of UV exposure time for different alkaline earth cations used as dopants.

doped films was found to increase with increase of GPTMS content of the Ormosil matrix (Figure 8a). The tungsten (W) content of the undoped films decreases for GPTMS percentages higher than 20%. On the other hand, the W

content of Ba^{2+} -doped sample increases continuously with increase in GPTMS content (Figure 8b), indicating more incorporation of the polyoxometalate species. A similar trend of phosphotungstate incorporation was observed using FTIR spectroscopy (Figure S1 in the Supplementary Information (SI) section). Therefore, the incorporation of both phosphotungstate and cations is clearly influenced by the composition of the hybrid matrix. The increased incorporation of the positively charged species in the films may be related to the presence of GPTMS derived chelating functional groups, such as oligo-ether chains and diols, which can complex the alkaline earth cations.^{50,51} The chelated cations might then electrostatically attract the $\text{PW}_{12}\text{O}_{40}^{3-}$ polyoxoanions, thus acting as nucleating sites for the formation of phosphotungstate-rich domains inside the hybrid matrix. Incorporation of the cations and subsequent adsorption of $\text{PW}_{12}\text{O}_{40}^{3-}$ on these nucleation sites seems to be the first step in the formation of such phosphotungstate-rich domains. The initially adsorbed

$\text{PW}_{12}\text{O}_{40}^{3-}$ polyoxoanions may further interact with other cations in the surrounding, such interaction being dependent on cation size. Again, the newly adsorbed cations may interact with more polyoxoanions in the surrounding. The overall result is an increased GPTMS/cations mediated incorporation of polyoxoanions in the hybrid films, as evidenced by XRF analysis. In the absence of cationic species, polyoxometalate incorporation is not effective because of the weak intermolecular interactions with the Ormosil matrices.

XRF analysis evidenced that the entrapment of phosphotungstate is enhanced by the presence of cations, possibly due to the electrostatic interactions between these species, suggesting it to be the possible reason for the superior photochromic response of cation-doped hybrid films. Such hypothesis is supported by the strong correlation between the photochromic response (Figure 6) and W $L\alpha$ intensity (Figure 8b) of Ba-doped films. Additionally, a linear correlation ($R^2 = 0.99$) is observed between photochromic response and W content (as indicated by W $L\alpha$ intensity) for the films doped with different alkaline earth cations (Figure 9). Since POMs tend to associate more favourably with larger cations^{52,53} due to their lower hydration radii and hydration energies,^{54,55} cation-phosphotungstate electrostatic interaction should follow the order $\text{Mg}^{2+} < \text{Ca}^{2+} < \text{Sr}^{2+} < \text{Ba}^{2+}$. This very same trend is observed in the XRF analysis and photochromism experiments (Figure 9). Therefore, the ion-size dependency observed for POM incorporation and the resulting enhanced photochromic response also fits with the electrostatic interaction based incorporation model.

Conclusions

Highly photochromic hybrid Ormosil-phosphotungstate materials were prepared using sol-gel route and the resulting hybrid materials were immobilized as multilayer films on glass substrate using dip-coating technique. The presence of GPTMS and alkaline earth metal cations leads to a significant enhancement (up to 7 times) of the photochromic response of the films by increasing the amount of phosphotungstate anions incorporated in the films. GPTMS provides the chelating sites for adsorption of cations and the cations in turn interact with phosphotungstate anions in the order: $\text{Mg}^{2+} < \text{Ca}^{2+} < \text{Sr}^{2+} < \text{Ba}^{2+}$. The photochromic response follows the same order indicating a correlation between cation size (or cation-phosphotungstate interaction) and photochromic response. The presence of GPTMS seems to prevent crystallization of the HPW leading

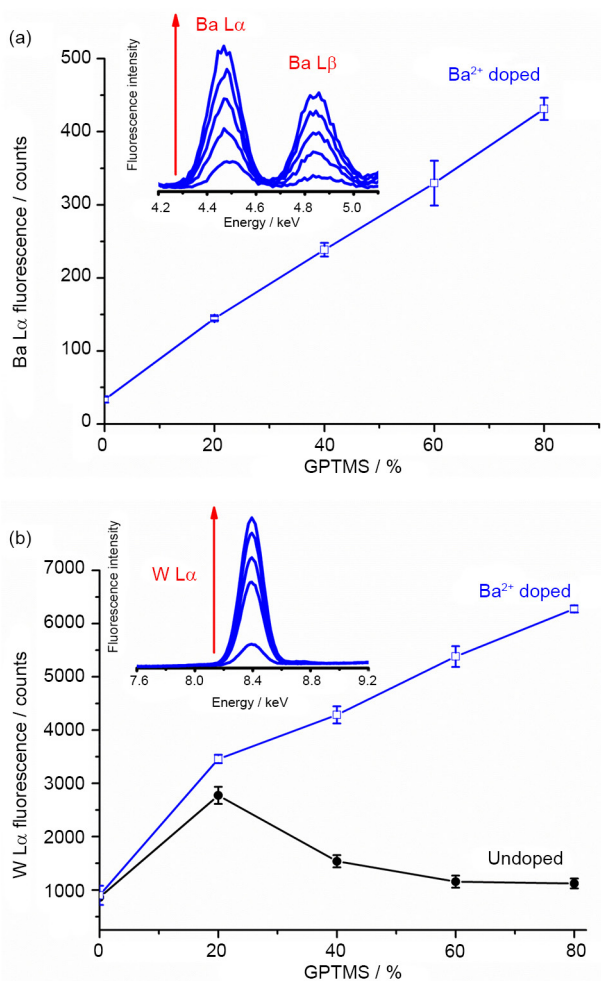


Figure 8. Increase in the barium (a) and tungsten (b) content of the Ba^{2+} -doped hybrids films as function of GPTMS content. The W content of the undoped film is also shown for comparison in (b).

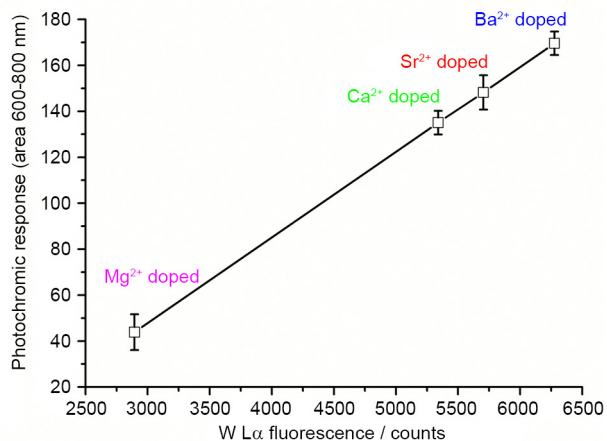


Figure 9. Correlation between the photochromic response and W content (fluorescence intensity) of the hybrid films (M80) for different doping cations. The % of GPTMS is 80% and UV exposure time is 10 min in each case.

to a homogeneous dispersion of the heteropolyanions in the hybrid films. The ion-size dependency observed for phosphotungstate's incorporation and the resulting enhancement of the photochromic response follow the electrostatic mediated incorporation model and can be extended to other POMs and metal cations.

Supplementary Information

Supplementary information is available free of charge at <http://jbcs.sbq.org.br> as PDF file.

Acknowledgements

The authors thank the São Paulo Research Foundation, FAPESP, research grant 2011/08120-0. Mateus B. Simões and Julia C. Noveletto thank the Coordenação de Aperfeiçoamento Pessoal de Nível Superior, CAPES for their fellowships. Elias P. Ferreira-Neto thanks FAPESP for PhD fellowship (2013/24948-3). Sajjad Ullah thanks The World Academy of Science (TWAS, Italy) and National Council for Scientific and Technological development (CNPq, Brazil) for PhD fellowship.

References

- Bouas-laurent, H.; Dürr, H.; *Pure Appl. Chem.* **2001**, *73*, 639.
- Irie, M.; *Chem. Rev.* **2000**, *100*, 1685.
- Pardo, R.; Zayat, M.; Levy, D.; *Chem. Soc. Rev.* **2011**, *40*, 672.
- Mills, A.; McFarlane, M.; Schneider, S.; *Anal. Bioanal. Chem.* **2006**, *386*, 299.
- Bianco, A.; Perissinotto, S.; Garbugli, M.; Lanzani, G.; Bertarelli, C.; *Laser Photonics Rev.* **2011**, *5*, 711.

- Bechinger, C.; Ferrere, S.; Zaban, A.; Sprague, J.; Gregg, B. A.; *Nature* **1996**, *383*, 608.
- Yoon, B.; Lee, J.; Park, I. S.; Jeon, S.; Lee, J.; Kim, J.-M.; *J. Mater. Chem. C* **2013**, *1*, 2388.
- Lebeau, B.; Innocenzi, P.; *Chem. Soc. Rev.* **2011**, *40*, 886.
- Pope, M. T.; Müller, A.; *Angew. Chem., Int. Ed. Engl.* **1991**, *30*, 34.
- Katsoulis, D. E.; *Chem. Rev.* **1998**, *98*, 359.
- Yamase, T.; *Chem. Rev.* **1998**, *98*, 307.
- He, T.; Yao, J.; *Prog. Mater. Sci.* **2006**, *51*, 810.
- Papaconstantinou, E.; *Chem. Soc. Rev.* **1989**, *18*, 1.
- Zhong, X.; Liu, Y.; Tang, X.; Wu, Q.; Li, L.; Yu, Y.; *Colloid Polym. Sci.* **2012**, *290*, 1683.
- Feng, W.; Ding, Y.; Liu, Y.; Lu, R.; *Mater. Chem. Phys.* **2006**, *98*, 347.
- Wang, C.; Zhou, B. P.; Zeng, X. P.; Hong, Y. Y.; Gao, Y. B.; Wen, W. J.; *J. Mater. Chem. C* **2015**, *3*, 177.
- Huang, F.-H.; Chen, C.-C.; Lin, D.-J.; Don, T.-M.; Cheng, L.-P.; *J. Nanopart. Res.* **2010**, *12*, 2941.
- Chen, Y.; Yu, G.; Li, F.; Xie, C.; Tian, G.; *J. Mater. Chem. C* **2013**, *1*, 3842.
- Štangar, U. L.; Orel, B.; Régis, A.; Colomban, P.; *J. Sol-Gel Sci. Technol.* **1997**, *8*, 965.
- Judeinstein, P.; Oliveira, P. W.; Krug, H.; Schmidt, H.; *Adv. Mater. Opt. Electron.* **1997**, *7*, 123.
- Ferreira-Neto, E. P.; Ullah, S.; de Carvalho, F. L. S.; de Souza, A. L.; de Oliveira Jr., M.; Schneider, J. F.; Mascarenhas, Y. P.; Jorge Jr., A. M.; Rodrigues-Filho, U. P.; *Mater. Chem. Phys.* **2015**, *153*, 410.
- De Oliveira, M.; de Souza, A. L.; Schneider, J.; Rodrigues-Filho, U. P.; *Chem. Mater.* **2011**, *23*, 953.
- Levy, D.; *Chem. Mater.* **1997**, *9*, 2666.
- Sanchez, C.; Lebeau, B.; Chaput, F.; Boilot, J.-P.; *Adv. Mater.* **2003**, *15*, 1969.
- Sanchez, C.; Belleville, P.; Popall, M.; Nicole, L.; *Chem. Soc. Rev.* **2011**, *40*, 696.
- Ferreira-Neto, E. P.; Carvalho, F. L. S.; Ullah, S.; Zoldan, V.; Pasa, A.; de Souza, A. L.; Battirolo, L.; Rudolf, P.; Bilmes, S.; Rodrigues-Filho, U. P.; *J. Sol-Gel Sci. Technol.* **2013**, *66*, 363.
- Pope, M. T.; *Heteropoly and Isopoly Oxometalates*; Springer-Verlag: Berlin, Heidelberg, 1983.
- Ferreira-Neto, E. P.; Ullah, S.; Ysnaga, O. A. E.; Rodrigues-Filho, U. P.; *J. Sol-Gel Sci. Technol.* **2014**, *72*, 290.
- Bao, H.; Wang, X.; Yang, G.; Li, H.; Zhang, F.; Feng, W.; *Colloid Polym. Sci.* **2014**, *292*, 2883.
- Fernandes, D.; Freire, C.; *J. Appl. Electrochem.* **2014**, *44*, 655.
- Jiang, M.; Wang, E.; Wei, G.; Xu, L.; Li, Z.; *J. Colloid Interface Sci.* **2004**, *275*, 596.
- Mialane, P.; Zhang, G.; Mbomekalle, I. M.; Yu, P.; Compain, J.-D.; Dolbecq, A.; Marrot, J.; Sécheresse, F.; Keita, B.; Nadjo, L.; *Chem. - Eur. J.* **2010**, *16*, 5572.

33. Qi, W.; Li, H.; Wu, L.; *J. Phys. Chem. B* **2008**, *112*, 8257.
34. Wang, Y.; Zeiri, O.; Sharet, S.; Weinstock, I. A.; *Inorg. Chem.* **2012**, *51*, 7436.
35. Hou, Y.; Zakharov, L. N.; Nyman, M.; *J. Am. Chem. Soc.* **2013**, *135*, 16651.
36. Pigga, J. M.; Liu, T.; *Inorg. Chim. Acta* **2010**, *363*, 4230.
37. Yin, P.; Li, D.; Liu, T.; *Chem. Soc. Rev.* **2012**, *41*, 7368.
38. Socrates, G.; *Infrared Characteristic Group Frequencies: Tables and Charts*, 3rd ed.; Wiley: London, UK, 2004.
39. Wencel, D.; Barczak, M.; Borowski, P.; McDonagh, C.; *J. Mater. Chem.* **2012**, *22*, 11720.
40. Lakshminarayana, G.; Nogami, M.; *J. Phys. Chem. C* **2009**, *113*, 14540.
41. Riegel, B.; Kiefer, W.; Hofacker, S.; Schottner, G.; *J. Sol-Gel Sci. Technol.* **2002**, *24*, 139.
42. Metroke, T. L.; Kachurina, O.; Knobbe, E. T.; *Prog. Org. Coat.* **2002**, *44*, 295.
43. Bridgeman, A. J.; *Chem. Phys.* **2003**, *287*, 55.
44. Fournier, M.; Feumi-Jantou, C.; Rabia, C.; Herve, G.; Launay, S.; *J. Mater. Chem.* **1992**, *2*, 971.
45. Mioč, U. B.; Dimitrijević, R. Ž.; Davidović, M.; Nedić, Z. P.; Mitrović, M. M.; Colomban, P.; *J. Mater. Sci.* **1994**, *29*, 3705.
46. Silviani, E.; Burns, R. C.; *J. Mol. Catal. A: Chem.* **2004**, *219*, 327.
47. Damjanović, L.; Rakić, V.; Mioč, U. B.; Auroux, A.; *Thermochim. Acta* **2005**, *434*, 81.
48. Staiti, P.; Freni, S.; Hocevar, S.; *J. Power Sources* **1999**, *79*, 250.
49. Song, Y.-F.; Long, D.-L.; Ritchie, C.; Cronin, L.; *Chem. Rec.* **2011**, *11*, 158.
50. Poonia, N. S.; Bajaj, A. V.; *Chem. Rev.* **1979**, *79*, 389.
51. Yanagida, S.; Takahashi, K.; Okahara, M.; *Bull. Chem. Soc. Jpn.* **1978**, *51*, 1294.
52. Grigoriev, V. A.; Cheng, D.; Hill, C. L.; Weinstock, I. A.; *J. Am. Chem. Soc.* **2001**, *123*, 5292.
53. Wang, Y.; Zeiri, O.; Sharet, S.; Weinstock, I. A.; *Inorg. Chem.* **2012**, *51*, 7436.
54. Marcus, Y.; *J. Chem. Soc., Faraday Trans.* **1991**, *87*, 2995.
55. Conway, B. E.; *Ionic Hydration in Chemistry and Biophysics (Studies in Physical & Theoretical Chemistry)*, 1st ed.; Elsevier Scientific Publishing Company: Amsterdam, NLD, 1981.

Submitted: July 14, 2015

Published online: October 27, 2015

FAPESP has sponsored the publication of this article.